

Shadowing Fading based Intersection Geographic Opportunistic Routing Protocol for Urban VANETs

Shuto Takahashi

Ritsumeikan University

Graduate School

of Inf. Sci. Eng.

is0361er@ed.ritsumei.ac.jp

Masami Yoshida

Ritsumeikan University

Graduate School

of Inf. Sci. Eng.

is0195hr@ed.ritsumei.ac.jp

Alberto Gallegos Ramonet

Ritsumeikan University

College of

Inf. Sci. Eng.

ramonet@fc.ritsumei.ac.jp

Taku Noguchi

Ritsumeikan University

College of

Inf. Sci. Eng.

noguchi@is.ritsumei.ac.jp

Abstract—In Vehicular Ad-hoc Networks (VANETs), the presence of many obstacles such as buildings and trees cause shadowing and fading, which interfere with the propagation of radio waves. However, most of the existing opportunistic routing protocols do not take into account shadowing in their simulations, which may lead to an overestimation of VANETs performance. To solve this problem, our proposed routing protocol can minimize the effect of shadowing by actively selecting street intersection nodes as relay nodes. In this study, we investigated the effect of shadowing on an existing routing protocol LSGO, using a shadowing obstacle model implemented ns-3. Additionally, we propose a Shadowing Fading based Intersection Geographic Opportunistic Routing Protocol (SIGO). SIGO determines the priority of a relay node by considering the distance between the relay node and the destination node, the link quality between these nodes, and a street Intersection Relay Index (IRI) in which the best relay node is selected according to the influence of shadowing. Through simulations, we confirmed the improvement of the packet delivery ratio and the decrease of the end-to-end delay and demonstrated the effectiveness of SIGO's communication performance.

Index Terms—VANET, Routing Protocols, Opportunistic Routing Protocols, Shadowing

I. INTRODUCTION

Intelligent Transportations Systems (ITS) [1] have been actively pursued to improve the safety and convenience of driving and reduce the environmental impact. Vehicle Ad-Hoc Networks (VANETs), which are formed by inter-vehicle communication, are essential for various applications in ITS. In VANETs, Ad-Hoc communication is achieved between vehicles equipped with wireless communication devices enabling the construction of flexible networks. When VANETs are deployed in urban environments, fast node mobility, heterogeneity, and the presence of buildings need to be considered in the performance evaluation. A wide variety of routing protocols has been proposed to meet various needs [2]. The existing routing protocols in VANETs can be classified into two categories: Topology-based routing protocols and geographic routing protocols. Topology-based routing protocols [3]–[5] use the network links information to forward packets. Additionally, these routing protocols are not suitable for VANETs because they cannot support fast node move-

ment. On the other hand, geographic routing protocols [6]–[15] can forward packets based on the neighboring nodes' location information and the destination node location. In this kind of routing protocols, nodes do not need to maintain established routes as in conventional mobile Ad-Hoc network routing protocols. Therefore, the geographic routing protocol can cope with topology changes with a small number of packets. Greedy forwarding is one of the most used packet forwarding methods in geographic routing protocols. However, in an actual urban environment, the drop rate of packets may increase due to shadowing and degradation of signal strength over distance. This increases the possibility of packet retransmission, resulting in increased overhead and end-to-end delay.

In contrast to these methods, opportunistic routing protocols have been attracting attention [16]. The main difference between opportunistic routing protocols and conventional routing schemes is that opportunistic routing protocols do not use a fixed route, but allow nodes that receive packets to decide whether or not to forward them. This can increase the chance of receiving packets and consequently achieve better performance than conventional routing schemes. However, most of the existing originally opportunistic routing protocols are not designed for urban environments, therefore their performance evaluation does not take into account the effect of shadowing fading caused by buildings and may result in an overestimating of the communication performance. In fact, it has been demonstrated that buildings attenuate the radio wave of 802.11p channels, and that the data transmission is limited alongside the road [17].

In this study, we evaluate the Link State aware Geographic Opportunistic routing protocol for VANETs (LSGO) [18], using an obstacle shadowing model [19]. Our evaluations tested LSGO under the obstacle shadowing model [19] using the ns-3 network simulator [20]. We also tested the protocol performance when shadowing is not considered. Additionally, we proposed a new routing protocol called Shadowing fading based Intersection Geographic Opportunistic routing protocol (SIGO) to improve the communication performance in shadowing environments. In the SIGO protocol, We consider the distance to the destination node and the expected transmission probability.

Furthermore, SIGO considers whether a node is close to a street intersection node when selecting relay nodes. Our evaluations demonstrated the effectiveness of the proposed method in a simulation environment. The rest of this paper is organized as follows: Section II describes the existing opportunistic routing protocols and shadowing. Section III describes LSGO, one of the most popular opportunistic routing protocols and problems with LSGO. Section IV describes the proposed method (SIGO), and Section V shows the performance evaluation and effectiveness of the proposed method. Finally, Section VI summarizes and discusses future work.

II. RELATED WORK

A. Opportunistic Routing Protocols Background

Recently, opportunistic routing protocols have attracted much attention. Compared with conventional geographic routing protocols [6], opportunistic routing protocols improve communication performance by increasing the number of opportunities for relay nodes to receive packets. The basic model of opportunistic routing protocols is shown in Figure 1.

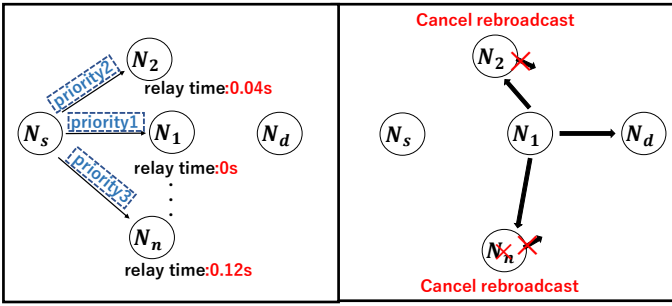


Fig. 1

The basic model of opportunistic routing protocols

The node N_s selects a candidate node for relaying and determines the priority from N_1 to N_n . After that, N_s writes the priorities of N_1 to N_n in the packet and broadcasts it. In each packet of the figure, the priority of the relay node is described for the sake of clarity, but the actual packet is broadcast, so the contents of the packet are identical. The nodes that received the packet set a relay timer according to their own priority. The higher the priority, the smaller the relay timer is set. The nodes that time out will rebroadcast packets. In addition, each relay node cancels its rebroadcast when it overhears the transmission of the packet from a node with a higher priority than itself before its timer expires, thereby preventing the increase of redundant packets. These results show that in opportunistic routing protocols, the priority determination algorithm directly impacts communication performance.

Opportunistic Multi-Hop Routing for Wireless Networks (ExOR) [16] has been proposed as a typical opportunistic routing protocol. It determines the priority of relay nodes by using an original Expected Transmission

Cost (ETX) [21]. However, this newly devised way to calculate the ETX value has a problem in that it does not take into account the random and fast mobility nature of nodes, which is a characteristic of VANETs nodes.

Therefore, LSGO devised a new ETX value suitable for VANETs. In LSGO, the ETX value is used as a metric to determine the priority, which improves the packet delivery ratio (PDR) and reduces the end-to-end delay. In the Collision Aware Opportunistic Routing Protocol (SCAOR) [22], to prevent packet collision that degrades network performance, node density is added as a metric in the priority determination. As a result, performance is improved compared to LSGO and EXOR in a highway deployment environment. In the Hybrid Opportunistic and Position-based Routing protocol for vehicular ad-hoc networks (OPBR) [23], to solve the problem of delay increase when the packet does not reach the relay node, OPBR infers the link breakage of the neighboring node from the location information gathered from the neighboring nodes.

However, one common issue in all of these protocols is that they do not take shadowing into account. This problem makes these protocols overestimate their communication performance. In Section III, we examine the impact of shadowing on the communication performance of LSGO using simulations.

B. Shadowing fading

When designing routing protocols for VANETs, many papers consider fast mobility of nodes, deviating node density, and link instability. However, VANETs are often assumed to be deployed in urban environments, therefore it is essential to design routing protocols that consider the effects of shadowing. As shown in Figure 2, the 802.11p channel commonly used in VANETs has a lower packet delivery ratio (PDR) in real-world measurements in the gray-zone [17] located on the side of the streets due to the influence of buildings.

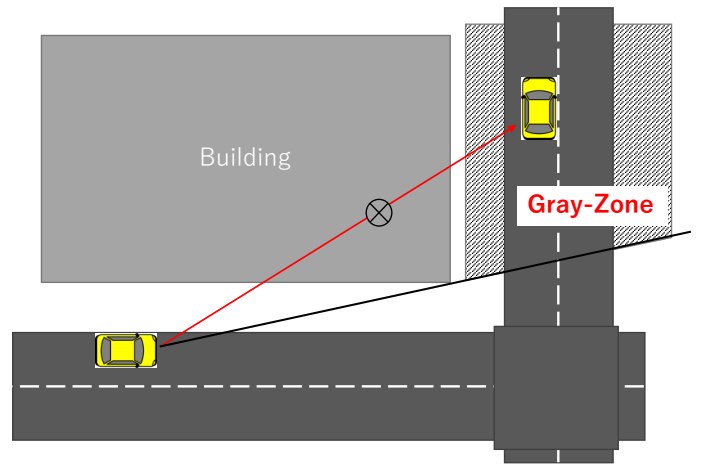


Fig. 2

The gray-zone in an intersection

Intersection-based selection routing protocols [24]–[26] are effective for these shadowing problems. The forwarding strategy of these protocols can be classified into three steps. The first one is intersection selection, the second one is road selection at the intersection, and the third one is forwarding on the selected road. In these intersection based routing approaches, the impact of shadowing fading can be minimized because packets are forwarded along the road. However, when packets are forwarded linearly, as shown in Figure 3, extra hop relays are introduced for each intersection in an intersection-based selection routing. These extra hop relays result in unnecessary relays and increasing the overall delay.

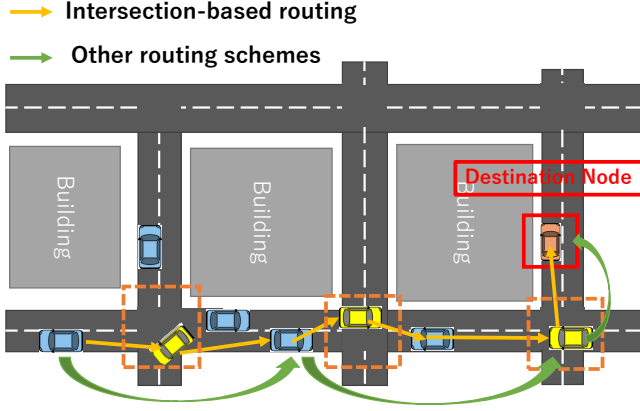


Fig. 3
Cases where intersection-based routing is inefficient

III. LSGO

In LSGO, each node periodically broadcasts a *hello* packet consisting of the node ID and its current position coordinate (x,y). The node that received the data packet selects some relay candidate nodes based on the information collected from neighboring nodes' hello packet to deliver the data packet to the destination node. Then, it assigns a priority to the selected candidate nodes and rebroadcasts the received packet. The transmitting node determines the priority of the candidate nodes according to the algorithm described below. In LSGO, the priority of relay candidate nodes is determined based on two metrics: link quality and distance to the destination. Each node that receives the data packet checks whether it contains its own ID, and discards the packet if it does not. The node checks its own priority and rebroadcasts the packet according to the priority scheduling algorithm if the ID is valid.

A. Link quality estimation

In LSGO, each node broadcasts a hello packet periodically, and they use the hello packets to measure the expected transmission probability of neighbor nodes. The transmitted hello packets consist of the node ID, and the node position coordinates (X,Y). To calculate the ETX of

a link, each node should record t_0 which means the time when the first hello packet is received and the number of packets it has received from the neighbor during the last w seconds. Then, according to the interval between t_0 and the current time t and the window w , the expected probability of successful transmission $r(t)$ is calculated by Equation (1)

$$r(t) = \begin{cases} \text{count}(t, t_0), & 0 < t - t_0 < 1, \\ \frac{\text{count}(t, t_0)}{(t - t_0)/\tau}, & 1 \leq t - t_0 \leq w \\ \frac{\text{count}(t - w, t)}{w/\tau}, & t - t_0 \geq w \end{cases} \quad (1)$$

The denominator is the number of hello packets that should have been received during the window, and τ represents the broadcast interval of the hello packets. $\text{count}(t, t_0)$ is the number of hello packets received during $t - t_0$. As can be seen from the equation, there are three situations in terms of the difference between $t - t_0$ and window time w . (1) $0 < t - t_0 < 1$, in this case, the packet delivery ratio is the number of hello packets received from t_0 to t . (2) $1 \leq t - t_0 < w$, the packet delivery ratio in this condition is the number of hello packets received from t_0 to t divided by the length of this period. (3) $t - t_0 \geq w$, in this situation, the calculation is the same as the calculation in the ETX metric.

In LSGO, the asymmetry of the link is not considered and only use the expected probability of one-way transmission to calculate the link ETX. Assuming that the expected probability of one-way transmission is $r(t)$, then the link ETX is calculated by Equation (2)

$$ETX = \frac{1}{r(t)^2} \quad (2)$$

B. Priority scheduling algorithm

LSGO uses a timer-based priority scheduling algorithm, in which the highest priority node sends the packet firstly. For other candidate nodes, if they hear a higher-priority node send a packet, they would not process the packet; if the timer expires and a higher-priority node is not transmitting, they would begin to send the packet. LSGO calculates the priority of node i according to Equation (3) below.

$$\frac{D_{sd} - D_{id}}{ETX_i^2}, D_{id} < D_{sd} \quad (3)$$

Where D_{sd} is the distance from the transmitting node to the destination node, and D_{id} is the distance from the candidate node i to the destination node. In addition, $D_{sd} - D_{id}$ is a distance metric. If the condition $D_{id} < D_{sd}$ is not satisfied, the node is excluded from the relay candidate nodes without calculating its priority. The larger the value calculated in Equation (3), the higher the priority of node i becomes.

C. Influence of shadowing

In this section, we explain the difference between the communication performance of LSGO with and without radio attenuation caused by shadowing.

1) *Simulation Settings*: The simulation parameters are shown in Table I. The simulation topology scenario was created using SUMO [27] as shown in Figure 4.

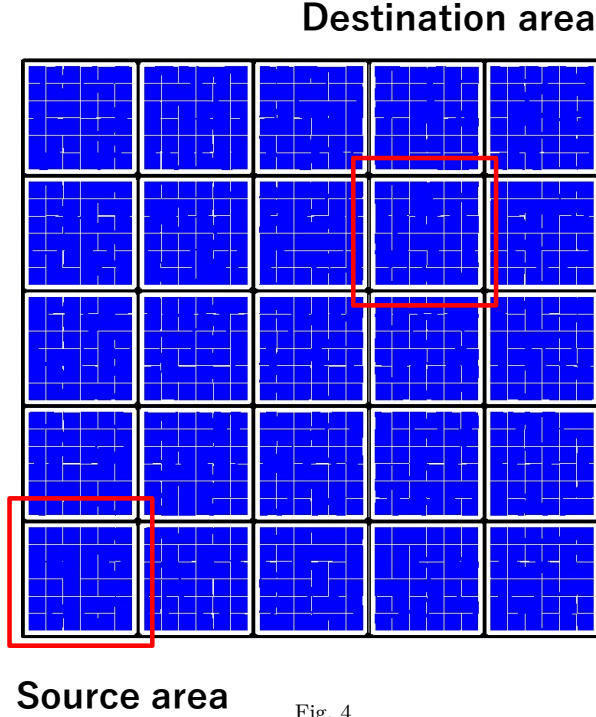


Fig. 4
simulation scenario

Ten source nodes and destination nodes pairs are randomly selected from the source area and destination area in Figure 4. Traffic signals are placed at each intersection, and buildings are placed as shown in the blue area of Figure 4. The obstacle shadowing model [19] is used as the radio wave propagation model. The obstacle shadowing propagation loss $L_{s,o}$ is calculated based on the loss for each wall and the distance (m) through the building as shown in Equation 4.

$$L_{s,o} = \alpha n + \beta d_0 \quad (4)$$

Where α is the attenuation per wall (dB), n is the number of walls penetrated. β is the attenuation per meter (dB), and d_0 is the distance traveled through obstacles (m). In this simulation experiment, $\alpha = 10\text{dB}$ and $\beta = 0.4\text{dB}$ were used in our evaluations. Although an optimized algorithm to select the number of relay candidate nodes was proposed in LSGO, the performance of this algorithm was poor when the shadowing propagation loss was used. This algorithm is constructed using the expected transmission probability ($r(t)$). Since the expected transmission probability is calculated from a hello packet, the packet

arrives with a higher probability than the transmission probability of the data packet with a larger data size. It is assumed that this is the reason for the performance degradation of the algorithm.

TABLE I
Simulation parameter

Simulator	NS-3 (v3.30)
Simulation area	1000m \times 1000m
Mobility model	Random mobility
Transmission range	250m
Number of vehicles	200, 300, 400
Radio Propagation Model	obstacle shadowing model [19]
MAC Layer	802.11p
Packet Size	512 byte
Simulation Time	30 s
hello interval	1 s
Window size w	10 s
Number of relay candidate nodes	5
shadowing parameter α	10db s
shadowing parameter β	0.4db

2) *Assessing the influence of shadowing*: The attenuation impact caused by the buildings on the communication performance of LSGO is evaluated in three evaluation categories: packet delivery ratio, end-to-end delay, and overhead.

Figure 5 shows the packet delivery ratio of the network simulator with and without using the obstacle shadowing loss propagation. The packet delivery ratio is the ratio of the total number of packets received by the destination node to the total number of packets sent by the source node. In Fig 5, when shadowing is considered in the simulation, the packet delivery ratio decreases for all number of nodes. This is presumably due to the decrease in the number of candidate nodes for relaying due to the radio attenuation caused by shadowing.

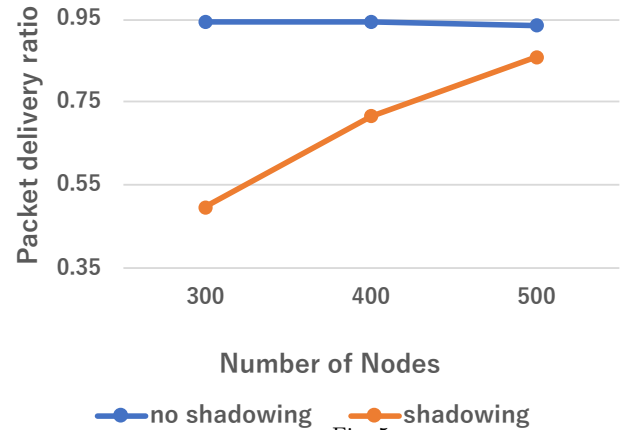


Fig. 5
Impact of shadowing: PDR

Figure 6 shows the end-to-end delay (s) of the network simulator with and without shadowing effects. The end-to-end delay is defined as the average time between the transmission of a packet by the source node and its successful reception by the destination node. In Figure

6, when shadowing is considered in the simulation, the end-to-end delay increases for all number of nodes. This is because the attenuation caused by shadowing, makes it difficult for packets to pass through the buildings to reach the destination node, making it difficult to form a linear path between the source and destination node.

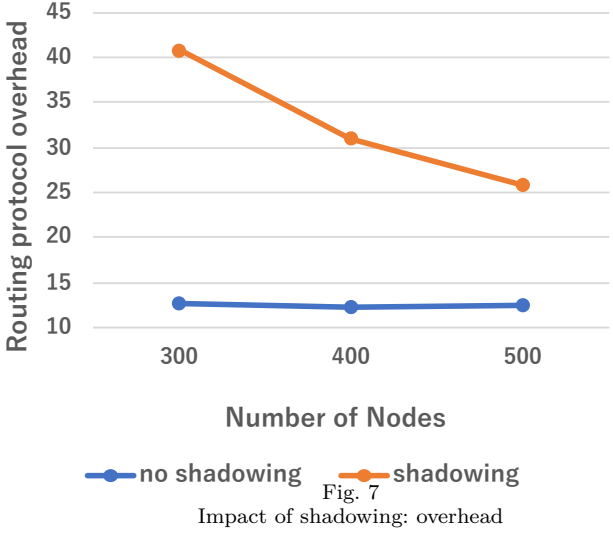
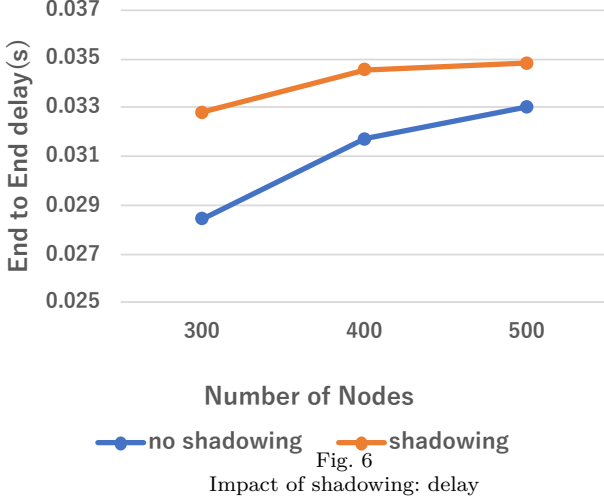


Figure 7 shows the overhead of LSGO with and without the shadowing effect. The overhead is the total number of data packets transmitted by all nodes in the entire network divided by the total number of data packets successfully received by the destination nodes. In Figure 7, the overhead increases for all number of nodes when shadowing is considered in the simulation. The algorithm works to cancel rebroadcast between relay candidate nodes according to their priority in opportunistic routing protocols. However, because of the shadowing effect, the possibility of not receiving the rebroadcast packet from high-priority nodes increases, and as a result, the overhead is assumed to have increased.

D. Problems with LSGO

In this section, we discuss the problems of the LSGO relay strategy. In the forwarding strategy of LSGO, a node that is closer to the destination node and has better link quality is more likely to be selected as a forwarding node. An example of this simulation is shown in Figure 8 (a). Consider the situation where node B is selected as a forwarding node shown in this Figure. In this case, the following relay nodes after node B (selected from nodes closer to the destination node than node B) are only nodes C and D with poor link quality due to shadowing. We call this problem the *local shadowing problem*. Occasionally, it is possible that the links with nodes C and D does not exist entirely due to shadowing. In those cases, the problem is that there is no longer a node close to the destination other than node B. This has long been a problem in location based routing protocols, and is called the local optimum problem. From the above, we can see that the

LSGO forwarding strategy is likely to fall into the local optimum problem and the local shadowing problem. This problem may be solved by selecting a street intersection node, such as node A, as a relay node, as shown in Figure 8 (b).

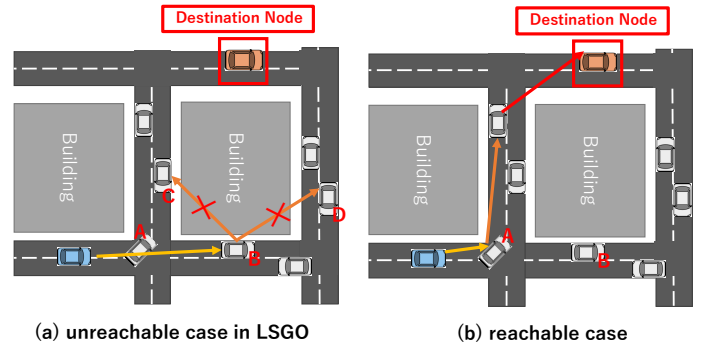


Fig. 8
Forwarding node selection problem

IV. THE PROPOSED SCHEME

In this study, we propose a new opportunistic routing protocol named SIGO, that takes street intersections into account. In SIGO, the priority of relay nodes is determined based on three metrics: distance to destination, link quality, and a street Intersection Relay Index (*IRI*) which is used to give priority to nodes in the intersection. The first two metrics: distance to destination and link quality, are calculated in the same way as in LSGO. In SIGO, as in LSGO, each node periodically broadcasts hello packets. To deliver the packets to the destination node, the transmitting node selects several relay candidate nodes among the neighboring nodes based on the information in the hello packets and broadcasts data packets containing the priority information of each relay candidate node.

The transmitting node determines the priority of the relay candidate nodes according to the algorithm described below. Each node that receives a data packet checks whether it contains its ID and discards the packet if it does not. If the ID is included, the node checks its priority and decides whether or not to rebroadcast the packet according to the *priority scheduling algorithm* described in section IV-E.

A. Basic assumption and terminology

In SIGO, we have made the following definition and assumptions.

- A *road segment* is defined as a part of the road which connects two unique street intersections.
- All nodes are equipped with GPS and have access to digital maps.
- Each node can identify the road segments and the street intersections where its neighbor nodes exist since it periodically receives hello packets from its neighbor nodes.

B. SIGO hello and data packet format

In SIGO, each node periodically broadcasts a hello packet to keep track of its neighbors' link quality and location. Figure 9 indicates the structure of the hello packet.

- ID : The identifier of the node that generates the hello packet.
- X : The x -coordinate value.
- Y : The y -coordinate value.
- v : The speed.
- a : The acceleration.
- θ : The direction.

The information of v , a , and θ are used in the *neighbor status prediction* algorithm described in subsection IV-D.

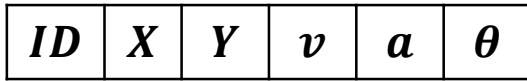


Fig. 9
The format of hello packet

The structure of the data packet is shown in Figure 10. It is assumed that some location information service is used to obtain the location information of the destination node, which is beyond the scope of this study. Since SIGO does not use control packets, the priority information assigned to each relay candidate node is included in the data packet.

- $SourceId$: The source node ID.
- $DstId$: The destination node ID.
- Dst_xPos : The x -coordinates of the destination node.
- Dst_yPos : The y -coordinates of the destination node.
- ID_i : The relay candidate node ID with priority i . $i = 1, 2, 3, \dots$ (highest to lowest Priority).
- $Data$: The data payload.

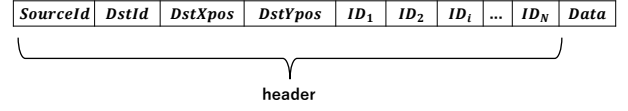


Fig. 10
The format of data packet

C. Intersection Relay Index (IRI)

In SIGO, a node i that received the data packet or the source node that generated the data packet calculates the *IRI* (intersection relay index) when the following two conditions are satisfied.

- A street intersection node is closer to the destination node than the source node or the node i .
- There is a street intersection node on an intersection adjacent to the road where the source node and node i exist.

The following procedures calculates *IRI* that gives priority to the street intersection node.

Step1: Selection of the closest road segment. To calculate *IRI*, the transmitting node (relay node i or the source node) selects one of the road segments closest to the destination node among the road segments where relay candidate nodes exist. To calculate the distance between the destination node and the road segment, the center coordinate of each road segment is used. An example is shown in Figure 11. The blue vehicle is the transmitting node, the yellow vehicles are the relay candidate nodes, the red vehicle is the destination node, and the green points are the center coordinates of each road segment. In this example, the road segment closest to the destination node is enclosed by the blue dashed line in the figure.

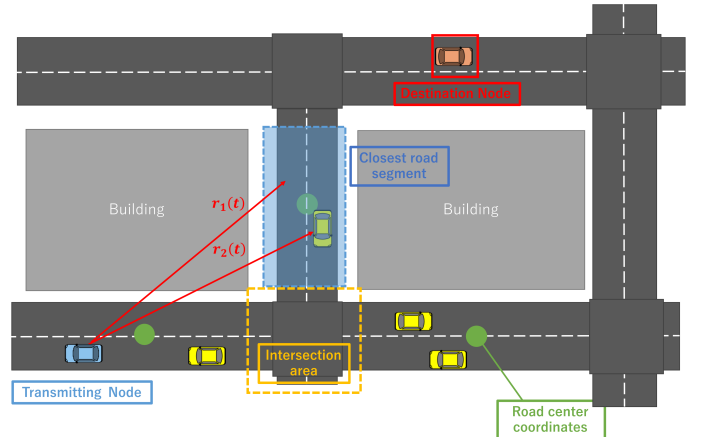


Fig. 11
The closest road segment

Step 2: Calculation of the transmission probability in a selected road segment. In this step, the transmitting node calculates the packet reachability probability R_p with that a packet reaches at least one

relay candidate node located in the closest road segment calculated in Step 1, using Equation 5.

$$R_p = 1 - \prod_{p=1}^N (1 - r_p(t)) \quad (5)$$

Where $r_p(t)$ is the expected transmission probability of the relay candidate node p ($1 \leq p \leq N$) in the road segment closest to the destination node. N represents the number of candidate nodes in the road segment closest to the destination node. The expected transmission probability is calculated using the same equation as in Equation 1.

Step3: Calculation of IRI . Using the R_p calculated in Step 2, the street Intersection Relay Index IRI is calculated using Equation 6.

$$IRI = \alpha \frac{90 \left(\frac{\theta_I}{90} \right)^{\frac{1}{\gamma}}}{R_p} \quad (6)$$

Where, θ_I is the angle between the lines connecting the transmitting node with the destination node and connecting the transmitting node and the intersection node (Figure 12). As θ_I increases and R_p decreases. As IRI increases, the transmitting node selects the intersection node as the relay node with a higher probability. The detailed operation of the relay node selection is described in Section IV-E. We also add a gamma correction to prevent the intersection node from being given too much priority when θ_I is small. γ is the gamma-correction value.

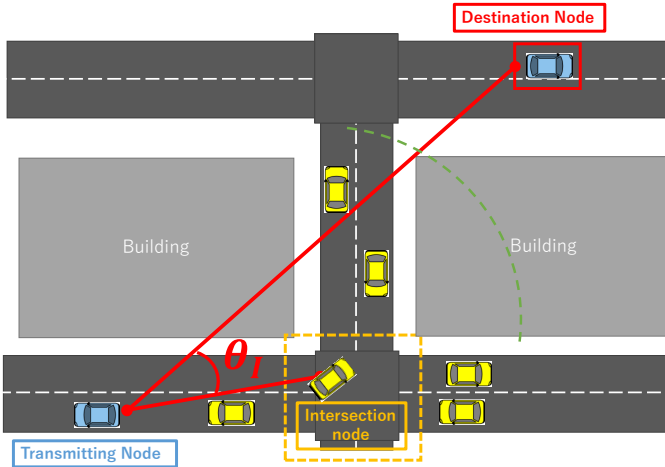


Fig. 12
The Intersection node angle

D. Neighbor status prediction algorithm

In most geographic routing protocols, each node obtains the location information of its neighboring nodes from the information in hello packets sent by neighboring nodes. However, the information in a hello packet may become outdated if the hello packet cannot be received or the transmission interval is long. Therefore, in SIGO, the

neighbor status prediction precisely identifies which roads or intersections neighboring vehicles exist. The neighbor status prediction algorithm improves the accuracy of the priority calculation of street intersection nodes and can remove the broken link nodes from the relay candidate nodes. This algorithm can be divided into two steps:

1) *Position prediction algorithm*: The transmitting node predicts the position of its selecting candidate node based on the information in the candidate node's hello packets. The predicted neighbor node's coordinates x' and y' are calculated by Equation 7.

$$\begin{cases} x' = x + \{v(t - t_l) + \frac{1}{2}a(t - t_l)^2\} \cos\theta, \\ y' = y + \{v(t - t_l) + \frac{1}{2}a(t - t_l)^2\} \sin\theta, \end{cases} \quad (7)$$

In this equation, a , v , and θ are the information in the hello packet received by the transmitting node at the time t_l . t is the current time.

2) *Prediction of broken links*: The transmitting node estimates the distance between itself and its neighboring node using the predicted position information and predicts the broken link node before transmitting the data packet. The transmitting node removes neighbor node i from the relay candidate nodes if the following condition is satisfied.

$$\sqrt{(x_s - x'_i)^2 + (y_s - y'_i)^2} > \maxRange \quad (8)$$

In this inequality, x_s and y_s are coordinates of the transmitting node, and x'_i and y'_i are coordinates of the neighbor node i . The left-hand side is the predicted distance between the transmitting node and the neighboring node at time t , and the right-hand side \maxRange is the threshold for detecting the link breakage.

E. Priority scheduling algorithm

In SIGO, a timer-based priority scheduling algorithm is used. In this algorithm, the node with the highest priority rebroadcasts the data packet first. When other relay candidate nodes overhear packets from nodes with a higher priority, they discard their pending packets. Each relay candidate node rebroadcasts the packet only when it had not received any packet from the node with higher priority than itself until its timer expired. In SIGO, the priority of node i is calculated by the following equations (9) and (10).

$$\frac{D_{sd} - D_{id}}{ETX_i^2} + IRI, D_{id} < D_{sd} \quad (9)$$

$$\frac{D_{sd} - D_{id}}{ETX_i^2}, D_{id} < D_{sd} \quad (10)$$

D_{sd} is the distance from the transmitting node to the destination node, and D_{id} is the distance from the relay candidate node i to the destination node. If the condition $D_{id} < D_{sd}$ is not satisfied, the node is excluded from the relay candidate nodes without calculating the priority. Equation (9) is applied when node i is a street intersection

node, and equation (10) is applied when node i is located outside of an intersection. The larger the value calculated by equation (9) or (10), the higher the priority is assigned to node i .

V. PERFORMANCE EVALUATION

To evaluate the usefulness of the proposed protocol, we compared it with the LSGO protocol in three evaluation items: packet delivery ratio (PDR), end-to-end delay, and overhead. The simulation scenario and settings were the same as in Section III-C. We evaluated the performance by varying the number of nodes and the shadowing parameter α in Equation 4. β was fixed to 0.4db. Figure 13 shows the PDR of SIGO and LSGO when the number of nodes and the shadowing parameter is varied. In this figure, the number in round brackets after the protocol name indicates the value of the shadowing parameter α . SIGO (10) shows the PDR of the proposed protocol when α is 10. As shown in figure 13, SIGO achieves a higher PDR than LSGO for all cases. As the number of nodes increases and the value of the shadowing parameter decreases, the PDR increases. This is because the possibility of forming an unreachable route (as shown in figure 8) increases in LSGO with an increase of α . While the possibility of forming a reachable route increases by prioritizing street intersection nodes in SIGO. We can also observe that the PDR of SIGO increases as the number of nodes increases compared to that of LSGO. It is assumed that this is due to the increase in the probability of the existence of nodes in the intersection. This is because the existence probability of intersection nodes increases according to the number of nodes.

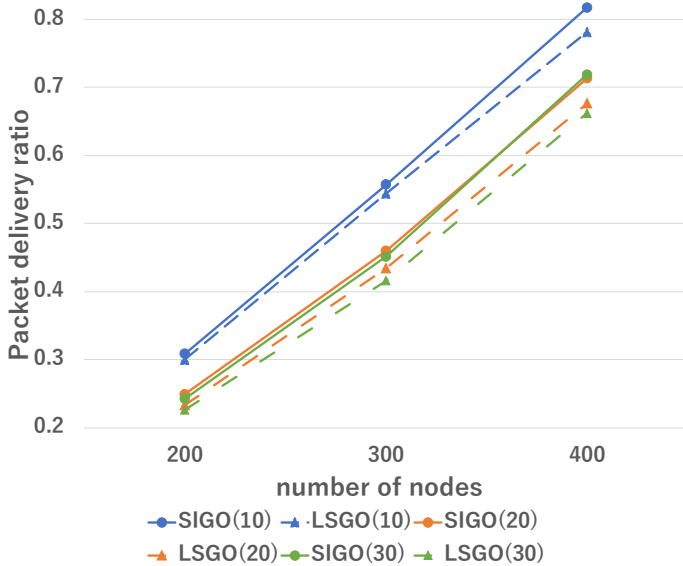


Fig. 13

Packet delivery ratio vs. number of nodes and shadowing intensity

Figure 14 shows the End-to-end delay of SIGO and LSGO when the number of nodes and the shadowing

parameter is varied. As shown in figure 14, the delay of both SIGO and LSGO increases with an increase in the number of nodes. In the simulation scenario and setting of this study, the effect of the proposed protocol on the delay is very small. We have the following three reasons for this: (1) Since the road structure used in our simulation is a grid, the distance between the source node and the destination node does not change regardless of which road the packet is relayed on. (2) In this experiment, we did not implement recovery routing such as GPSR recovery scheme to deal with the local optimum problem. (3) Retransmission control is not used in this experiment.

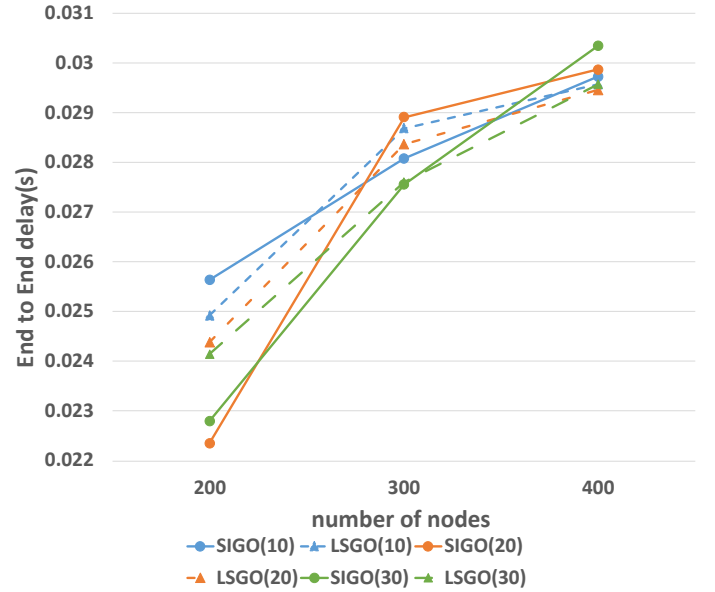


Fig. 14

End-to-end delays vs. number of nodes and shadowing intensity

Figure 15 shows the overhead of SIGO and LSGO when the number of nodes and the shadowing parameter are varied. Figure 15 tells us three characteristics: (1) The overhead of both LSGO and SIGO decreases with an increase in the number of nodes; (2) The overhead improvement of SIGO over LSGO increases with an increase in the shadowing parameter; (3) The difference in overhead between SIGO and LSGO becomes smaller with an increase in the number of nodes. The reason for (1) is that the total number of data packets successfully received by the destination node increases for both LSGO and SIGO, increasing the number of nodes. The reason for (2) is that the total number of data packets successfully received by the destination node increases in SIGO than in LSGO, increasing the shadowing parameter. In addition, this means that even though the total number of data packets successfully received by destination nodes increases in SIGO, the total number of data packets transmitted by all nodes does not increase significantly compared to LSGO. The reason for (3) is that when the number of nodes is large, rebroadcasting by the intersection node does not

always result in efficient communication. Suppose there is a building in the direction of the destination node and a street intersection node rebroadcasts the packet in SIGO. In that case, nodes on two different roads forming the intersection are likely to be selected as relay candidate nodes when the number of nodes large. In this situation, the possibility that a low priority candidate node cannot receive packets from a high-priority relay candidate node due to the shadowing effect of a building increases. As a result, redundant rebroadcasting increases because the rebroadcasting by a low-priority relay candidate node is not canceled. Figure 16 shows an example of this situation. The packets rebroadcasted by the street intersection node are received by nodes 1-4. Nodes 1, 2, 3, and 4 have a higher priority in that order. Ideally, only node 1 should rebroadcast the data packet. However, even if node 1 rebroadcasts the packet, nodes 3 and 4 cannot receive it due to the shadowing effect and rebroadcast.

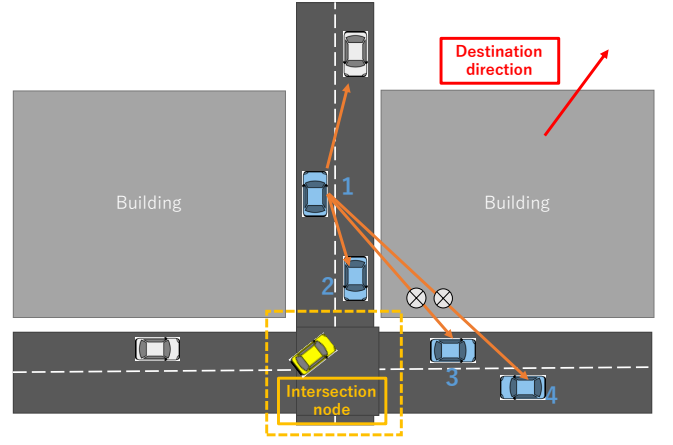


Fig. 16
Causes of increased overhead

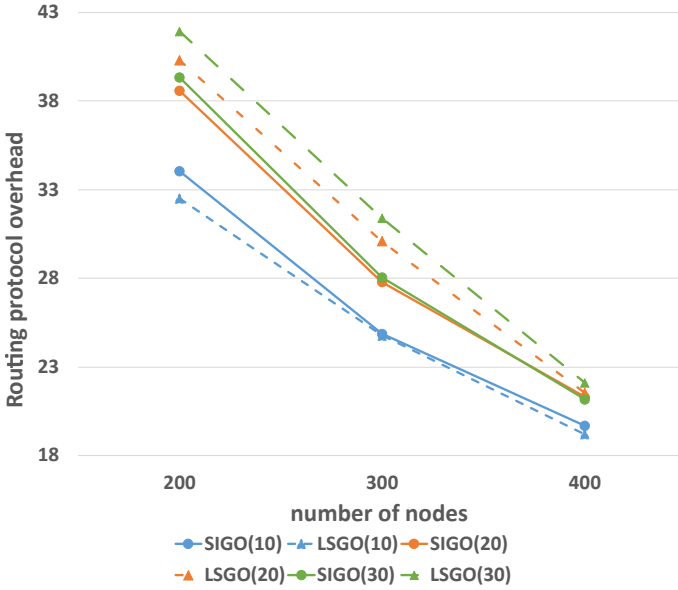


Fig. 15
Routing protocol overhead vs. number of nodes and shadowing intensity

VI. CONCLUSION

In this study, we evaluated an existing opportunistic routing protocol under the impact of shadowing in simulation. We demonstrated that the existing routing protocol degrades the communication performance when the effect of shadowing fading is taken into account by simulation. We also proposed SIGO, which forms routes that are less susceptible to shadowing, and showed its effectiveness by improving the packet delivery ratio and reducing the overhead. Future work includes optimizing the number of relay candidate nodes, which was set to a fixed value in our experiments. Furthermore, we plan to evaluate more complex simulation scenarios and redesign the SIGO routing protocol to support various scenarios.

REFERENCES

- [1] L. Figueiredo, I. Jesus, J. Machado, J. Ferreira, and J. Martins de Carvalho, "Towards the development of intelligent transportation systems," *ITSC 2001. 2001 IEEE Intelligent Transportation Systems. Proceedings (Cat. No. 01TH8585)*, pp. 1206–1211, 2001.
- [2] A. D. Devangavi and R. Gupta, "Routing protocols in vanet — a survey," pp. 163–167, 2017.
- [3] C. Perkins and E. Royer, "Ad-hoc on-demand distance vector routing," *Proceedings WMCSA '99. Second IEEE Workshop on Mobile Computing Systems and Applications*, pp. 90–100, 1999.
- [4] D. B. Johnson, D. A. Maltz, J. Broch *et al.*, "Dsr: The dynamic source routing protocol for multi-hop wireless ad hoc networks," *Ad hoc networking*, vol. 5, no. 1, pp. 139–172, 2001.
- [5] T. Clausen, P. Jacquet, C. Adjih, A. Laouiti, P. Minet, P. Muhlethaler, A. Qayyum, and L. Viennot, "Optimized link state routing protocol (olsr)," 2003.
- [6] B. Karp and H.-T. Kung, "Gpsr: Greedy perimeter stateless routing for wireless networks," *Proceedings of the 6th annual international conference on Mobile computing and networking*, pp. 243–254, 2000.
- [7] C. Lochert, M. Mauve, H. Füller, and H. Hartenstein, "Geographic routing in city scenarios," *ACM SIGMOBILE mobile computing and communications review*, vol. 9, no. 1, pp. 69–72, 2005.
- [8] K. C. Lee, J. Härri, U. Lee, and M. Gerla, "Enhanced perimeter routing for geographic forwarding protocols in urban vehicular scenarios," *2007 IEEE Globecom Workshops*, pp. 1–10, 2007.
- [9] V. Naumov and T. R. Gross, "Connectivity-aware routing (car) in vehicular ad-hoc networks," pp. 1919–1927, 2007.
- [10] S. Schnauffer and W. Effelsberg, "Position-based unicast routing for city scenarios," *2008 International Symposium on a World of Wireless, Mobile and Multimedia Networks*, pp. 1–8, 2008.
- [11] M. Jerbi, S.-M. Senouci, T. Rasheed, and Y. Ghamri-Doudane, "Towards efficient geographic routing in urban vehicular networks," *Ieee transactions on vehicular technology*, vol. 58, no. 9, pp. 5048–5059, 2009.
- [12] K. Shafiee and V. C. Leung, "Connectivity-aware minimum-delay geographic routing with vehicle tracking in vanets," *Ad Hoc Networks*, vol. 9, no. 2, pp. 131–141, 2011.
- [13] S.-H. Cha, K.-W. Lee, and H.-S. Cho, "Grid-based predictive geographical routing for inter-vehicle communication in urban areas," *International Journal of Distributed Sensor Networks*, vol. 8, no. 3, p. 819497, 2012.
- [14] T.-Y. Wu, Y.-B. Wang, and W.-T. Lee, "Mixing greedy and predictive approaches to improve geographic routing for vanet," *Wireless Communications and Mobile Computing*, vol. 12, no. 4, pp. 397–378, 2012.

- [15] Y. Xu, L. Wang, and Y. Yang, "Dynamic vehicle routing using an improved variable neighborhood search algorithm," *Journal of Applied Mathematics*, vol. 2013, 2013.
- [16] S. Biswas and R. Morris, "Exor: Opportunistic multi-hop routing for wireless networks," *Proceedings of the 2005 conference on Applications, technologies, architectures, and protocols for computer communications*, pp. 133–144, 2005.
- [17] F. Lv, H. Zhu, H. Xue, Y. Zhu, S. Chang, M. Dong, and M. Li, "An empirical study on urban ieee 802.11 p vehicle-to-vehicle communication," *2016 13th Annual IEEE International Conference on Sensing, Communication, and Networking (SECON)*, pp. 1–9, 2016.
- [18] X. Cai, Y. He, C. Zhao, L. Zhu, and C. Li, "Lsgo: link state aware geographic opportunistic routing protocol for vanets," *EURASIP Journal on wireless communications and networking*, vol. 2014, no. 1, pp. 1–10, 2014.
- [19] S. E. Carpenter and M. L. Sichitiu, "An obstacle model implementation for evaluating radio shadowing with ns-3," *Proceedings of the 2015 Workshop on Ns-3*, pp. 17–24, 2015.
- [20] G. Carneiro, "Ns-3: Network simulator 3," *UTM Lab Meeting April*, vol. 20, pp. 4–5, 2010, <https://www.nsnam.org>.
- [21] D. S. De Couto, D. Aguayo, J. Bicket, and R. Morris, "A high-throughput path metric for multi-hop wireless routing," *Proceedings of the 9th annual international conference on Mobile computing and networking*, pp. 134–146, 2003.
- [22] V. Sadatpour, F. Zargari, and M. Ghanbari, "A collision aware opportunistic routing protocol for vanets in highways," *Wireless Personal Communications*, vol. 109, no. 1, pp. 175–188, 2019.
- [23] A. Ghaffari, "Hybrid opportunistic and position-based routing protocol in vehicular ad hoc networks," *Journal of Ambient Intelligence and Humanized Computing*, vol. 11, no. 4, pp. 1593–1603, 2020.
- [24] T. Darwish and K. A. Bakar, "Traffic aware routing in vehicular ad hoc networks: characteristics and challenges," *Telecommunication systems*, vol. 61, no. 3, pp. 489–513, 2016.
- [25] N. Mirjazaee and N. Moghim, "An opportunistic routing based on symmetrical traffic distribution in vehicular network," *Computers & Electrical Engineering*, vol. 47, pp. 1–12, 2015.
- [26] K. N. Qureshi, A. H. Abdullah, and A. Altameem, "Road aware geographical routing protocol coupled with distance, direction and traffic density metrics for urban vehicular ad hoc networks," vol. 92, no. 3, pp. 1251–1270, 2017.
- [27] L. B.-W. J. E. Y.-P. F. R. H. L. L. J. R. P. W. Pablo Alvarez Lopez, Michael Behrisch and E. Wießner, "Microscopic traffic simulation using sumo," *2019 IEEE Intelligent Transportation Systems Conference (ITSC)*, vol. 20, pp. 2575–2582, 2018.